μg/ml) for 1 hour at room temperature with gentle shaking. Filters were washed three times for 10 min in TNE25 (250 ml) and were subjected to autoradiography with DuPont intensifying screens.
29. E. Quakenbush *et al*, *Proc. Natl. Acad. Sci U.S.A.* **84**, 6526 (1987).
30. S. Koizumi *et al.*, *Oncogene* **5**, 675 (1990).
31. L. M. Staudt *et al.*, *Science* **241**, 577 (1988).
32. S. Fujiwara *et al.*, *Mol. Cell. Biol.* **8**, 4700 (1988).
33. M. J. R. Stark, *Gene* **51**, 255 (1987).
34. M. S. Parmacek and J. M. Leiden, *J. Biol. Chem.* **264**, 13217 (1989).
35. K. Leung and G. J. Nabel, *Nature* **333**, 776 (1988).
36. The authors thank D. Ginsburg and G. Nabel for critical review of the manuscript. We also acknowledge S. Fujiwara and S. Koizumi for providing the anti-Ets MAbs used in these studies. We thank B. Burck for preparation of the illustrations and J. Pickett for expert secretarial assistance. Supported in part by Public Health Service grant AI-29673. T.L. is a Special Fellow of the Leukemia Society of America.

11 May 1990; accepted 31 August 1990

A Map of Visual Space Induced in Primary Auditory Cortex

ANNA W. ROE, SARAH L. PALLAS, JONG-ON HAHM, MRIGANKA SUR*

Maps of sensory surfaces are a fundamental feature of sensory cortical areas of the brain. The relative roles of afferents and targets in forming neocortical maps in higher mammals can be examined in ferrets in which retinal inputs are directed into the auditory pathway. In these animals, the primary auditory cortex contains a systematic representation of the retina (and of visual space) rather than a representation of the cochlea (and of sound frequency). A representation of a two-dimensional sensory epithelium, the retina, in cortex that normally represents a one-dimensional epithelium, the cochlea, suggests that the same cortical area can support different types of maps. Topography in the visual map arises both from thalamocortical projections that are characteristic of the auditory pathway and from patterns of retinal activity that provide the input to the map.

THE MECHANISMS BY WHICH SENSORY maps form in the neocortex remain an outstanding question in cortical development. There is evidence that both the cortical target tissue (*1*) and sensory information from peripheral receptors (*2*) are important in the mapping process. We have addressed the question by using a preparation in which fibers from the retina are directed into the auditory pathway in ferrets. In particular, we asked whether primary auditory cortex, which normally contains a representation of the cochlea, would now contain a systematic map of the retina and of visual space. We reasoned that a map of the visual field in primary auditory cortex, if it were to exist, would also provide important clues to how cortical targets and sensory inputs contribute to generating maps of sensory surfaces in the cortex.

To route visual projections to auditory cortex, the retina is deprived of its two major targets by surgical lesions in neonatal ferret kits. One target, the superior colliculus, is ablated directly, while the other target, the lateral geniculate nucleus (LGN), atrophies severely by retrograde degeneration after ablation of visual cortex. Concurrently, ascending auditory fibers to the medial geniculate nucleus (MGN), the principal auditory thalamic nucleus, are sectioned in the brachium of the inferior colliculus. Retinal afferents then project into the deafferented MGN (*3*); in lesioned animals reared to adulthood, neurons with well-defined visual responses can be recorded in this nucleus and from its main cortical target, the primary auditory cortex (*4*).

We have now examined the map of the visual field induced in primary auditory cortex in lesioned animals. Adult ferrets ($n = 7$), operated on at birth as described above, were prepared for electrophysiological recording (*5*). A grid of electrode penetrations was made in primary auditory cortex. We plotted receptive fields of visual cells recorded in cortex on a tangent screen using flashing or moving spots or bars of light. We identified recording sites as lying within primary auditory cortex by matching lesions made during recording with borders defined histologically (*6*).

Cortical recording sites and corresponding visual receptive field locations from an adult ferret in which retinal projections were induced into the auditory pathway are shown in Fig. 1. Receptive fields close to the vertical midline of the visual field are represented at the medial edge of primary auditory cortex (Fig. 1, A to C; receptive fields 1 and 2), and more peripheral parts of the visual field lie progressively laterally in cortex. Several receptive field sequences (Fig. 1, B and C) show that lower visual field elevations are represented posteriorly in cortex, and receptive fields move upward in elevation as recording sites move anteriorly across cortex.

We have quantified several aspects of the map. The map is retinotopic overall, although there is some variability in receptive field location (*7*). Azimuths increase systematically with mediolateral distance on the cortex (Pearson's coefficient of correlation, $r = 0.74$, $P < 0.01$), while elevations increase from posterior to anterior ($r = 0.46$, $P < 0.05$). Mapping indices (*7*) that compare actual locations with theoretical ones for a perfectly retinotopic map indicate that azimuths are mapped more precisely than elevations (*8*). Magnification (*9*) is relatively constant across the map (Fig. 1D), suggesting a linear mapping of the retina on cortex (*10*).

The map shown in Fig. 1 is an example of the maps we have recorded in primary auditory cortex in four lesioned animals. The representation of azimuth is stereotypical in all maps, increasing from medial to lateral in cortex. Furthermore, the representation of azimuth is consistently more precise than the representation of elevation (*11*). Indeed, the polarity of the elevation representation can reverse in some animals so that elevations either increase from posterior to anterior in cortex (as shown in Fig. 1; three animals) or from anterior to posterior (data not shown; one animal).

We regard these observations as significant for understanding how sensory maps form in the cortex. Our results demonstrate that the form of the map is not an intrinsic property of the cortex and that a cortical area can come to support different types of maps. In normal ferrets, primary auditory cortex contains a representation of the cochlea (*12*), with low sound frequencies represented laterally and high frequencies medially in cortex; the mediolateral dimension thus constitutes the variable-frequency axis in cortex. Neurons along the anteroposterior dimension in primary auditory cortex all represent the same sound frequency and constitute the isofrequency axis (*13*). In lesioned ferrets, a systematic representation of the retina and of visual space occupies both the mediolateral and anteroposterior dimensions of cortex. Thus, cortex that normally represents a one-dimensional (1-D) sensory epithelium (the cochlea) can, after early developmental manipulations, represent topographically a two-dimensional (2-D) epithelium (the retina).

The mechanisms by which topography is

Department of Brain and Cognitive Sciences, Massachusetts Institute of Technology, Cambridge, MA 02139.

*To whom correspondence should be addressed at Department of Brain and Cognitive Sciences, E25-618, Massachusetts Institute of Technology, Cambridge, MA 02139.

established in the dimensions of azimuth and elevation of the visual map are likely to be different. The normal pattern of projections from the MGN to primary auditory cortex (*14*) is highly topographic along the variable frequency axis but rather convergent and divergent [within the excitatory-excitatory (EE) and excitatory-inhibitory (EI) systems (*15*)] along the isofrequency axis (Fig. 2). Thus, in lesioned animals, the existing thalamocortical organization along the mediolateral or "variable frequency" dimension of cortex would lead to topography along the azimuthal axis of the visual map (*16*). However, along the anteroposterior or "isofrequency" dimension of cortex, the highly overlapped thalamocortical connections would not, alone, predict topographic mapping of visual field elevation. Consistent with this anisotropy in thalamocortical connections that is characteristic of the auditory pathway, we find that the mapping of azimuths in the visual map is more precise than the mapping of elevations. The visual map in primary auditory cortex of lesioned ferrets thus differs from the visual map in primary visual cortex of normal ferrets (*17*), where elevations are mapped as precisely as azimuths and where the map arises from retinal input relayed through the visual thalamus to cortex along projections that are topographic along both axes of representation (Fig. 2).

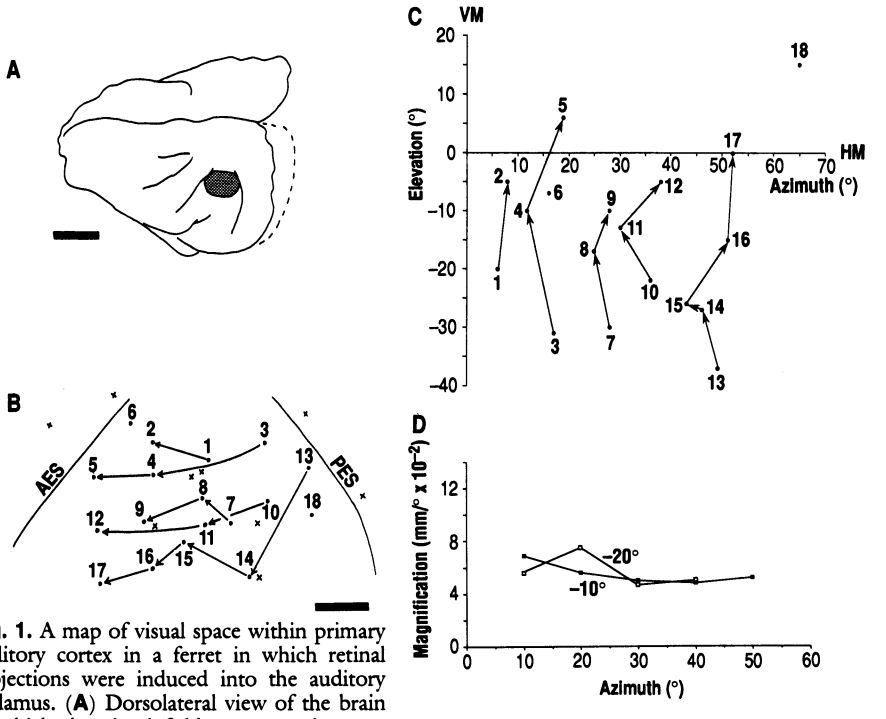

Fig. 1. A map of visual space within primary auditory cortex in a ferret in which retinal projections were induced into the auditory thalamus. (**A**) Dorsolateral view of the brain in which the visual field representation was mapped in primary auditory cortex (shown as stippled area on the brain). The dotted line represents the portion of visual cortex that was ablated at birth in this animal. Scale bar, 5 mm. (**B**) A detailed view of the recording sites within primary auditory cortex. Sites marked by an x denote penetrations in which no visual receptive field could be mapped. AES, anterior ectosylvian sulcus; PES, posterior ectosylvian sulcus. Scale bar, 1 mm. (**C**) Progressions of receptive field centers corresponding to rows of recording sites shown in (B). For clarity, the receptive fields themselves are not drawn. Receptive field diameters ranged from 4° to 20°. VM, vertical meridian; HM, horizontal meridian. (**D**) Linear magnification factors as a function of azimuthal eccentricity in the map. Factors derived along two isoelevation lines (at −10° and −20°) are shown.

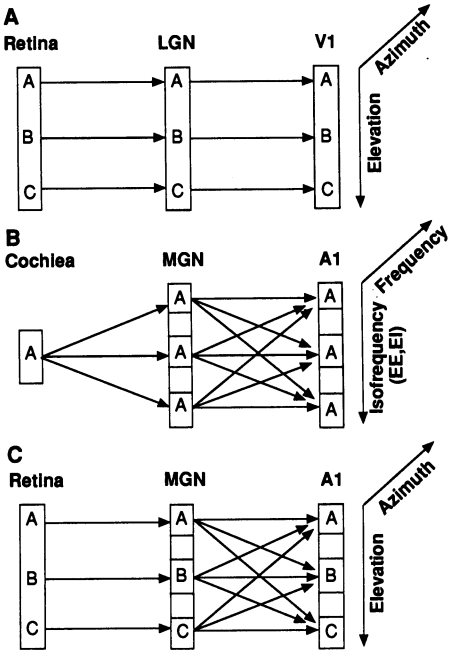

Fig. 2. Schematic representation and summary of projections from the sensory receptor surface through the thalamus to cortex in (A) the normal visual system, (B) the normal auditory system, and (C) lesioned ferrets with retinal projections induced into the auditory pathway. (**A**) In the visual pathway, each point on the retina projects in a roughly point-to-point fashion through the LGN to primary visual cortex (V1). Thus, a 2-D map of visual space exists in V1 (indicated schematically by arrows showing the mapping of visual field azimuth and of elevation along orthogonal axes on the cortex). (**B**) In the auditory pathway, each point on the cochlea projects, through intermediate relays, to a slab of cells along the isofrequency axis in the MGN. Each isofrequency slab in the MGN projects in highly overlapping fashion to its corresponding isofrequency slab in primary auditory cortex (A1). The cortex thus contains a 1-D map of the cochlea along the variable frequency axis (marked "frequency"). [Within the isofrequency axis in MGN and A1, separate clusters of neurons receive either excitation from both ears (EE neurons) or excitation from the contralateral ear and inhibition from the ipsilateral ear (EI neurons). Each EE (or EI) slab in the MGN projects to all of the EE (or EI) slabs in A1 (*15*)]. (**C**) In lesioned ferrets, we induce input from the retina, a 2-D sensory surface, into the MGN and find a 2-D visual map in A1, despite the fact that "isofrequency" slabs in the MGN still project to A1 in an overlapped way (*6*). See text for details.

At least two mechanisms may be responsible for establishment of topography in the axis of elevation of the visual map in auditory cortex. One possibility is that thalamocortical projections are more spatially restricted in the anteroposterior dimension in lesioned ferrets than in normal animals (*18*). However, retrograde labeling techniques used to study thalamocortical projections in both normal and lesioned ferrets indicate that the projections are substantially similar (*6*). A second possibility is that visual input, characterized by specific patterns of retinal activity (*19*), leads in the cortex to physiological selection of subsets of thalamic input from a potentially large set of inputs available anatomically (*20*). It has been proposed that selection of inputs occurs along the isofrequency axis in normal auditory cortex (*21*), and selection based on correlations in input activity may underlie the generation and maintenance of maps in the normal somatosensory and visual cortex as well (*22*). Regardless of mechanism, the presence of a map of visual space in auditory cortex indicates that functional topography in a cortical map is regulated significantly by the sensory receptor sheet during development.

REFERENCES AND NOTES

1. I. Kaiserman-Abramov, A. Graybiel, W. H. Nauta, *Neuroscience* **5**, 41 (1983); J. Olavarria and R. C. Van Sluyters, *J. Comp. Neurol.* **230**, 249 (1984); R. Guillery, M. Ombrellaro, A. LaMantia, *Dev. Brain Res.* **20**, 221 (1985); P. Rakic and R. W. Williams, *Soc. Neurosci. Abstr.* **12**, 1499 (1986); D. Dawson and H. Killackey, *Dev. Brain Res.* **17**, 309 (1985). See, for review, P. Rakic, *Science* **241**, 170 (1988).
2. H. Van der Loos and J. Dorfl, *Neurosci. Lett.* **7**, 23 (1978); J. H. Kaas and R. W. Guillery, *Brain Res.* **59**, 61 (1975).

3. G. E. Schneider, *Brain Behav. Evol.* **8**, 73 (1973); D. O. Frost, *J. Comp. Neurol.* **203**, 227 (1981).
4. M. Sur *et al.*, *Science* **242**, 1437 (1988).
5. Four animals were mapped extensively and form the basis for this report. Procedures for preparing the animals for physiological recording were similar to those we have used previously (*4*). Animals were anesthetized with ketamine (30 mg of body weight per kilogram) and xylazine (2 mg/kg) and paralyzed with gallamine triethiodide (10 mg/kg per hour); their respiration was artificially controlled. Anesthesia was continuously monitored and maintained. End-tidal CO_2 was maintained at 4%. Parylene-insulated tungsten microelectrodes were used to record unit activity mostly in the middle layers of primary auditory cortex.
6. S. L. Pallas *et al.*, *J. Comp. Neurol.* **298**, 50 (1990).
7. We examined retinotopy and variability in the map in two ways. First, we plotted the azimuth of each receptive field against the mediolateral distance of the recording site from the medial edge of primary auditory cortex (and, separately, elevation against anteroposterior distance from the posterior edge of auditory cortex) and calculated a Pearson coefficient of correlation (r) along with the associated probability of departure from a random mapping. The coefficient of correlation was used because the variables under consideration, visual field azimuth (or elevation) and cortical distance, are essentially random samples from a bivariate distribution. Second, we defined a mapping index for azimuth (and separately for elevation) as the mean, over all recording sites, of |(actual value of receptive field azimuth − ideal value)|/(maximum value of azimuth represented − minimum value). We determined ideal azimuth and elevation values by overlaying isoazimuth and isoelevation lines over the mapped cortical region. The mapping index (for azimuth and elevation) would be 0 for a perfectly retinotopic map and close to 1 for a map without any topographic order.
8. For the map shown in Fig. 1, the mapping indices (±SEM) are 0.052 (±0.012) for azimuth and 0.124 (±0.055) for elevation.
9. Smoothed isoazimuth and isoelevation lines were fitted to the experimental data. Linear magnification factors, defined as the distance of cortex that represents a unit distance of visual field, were measured along a given isoelevation line as the extent of cortex representing each successive 10° of azimuth.
10. This is consistent with the demonstration that retinal W cells, which are distributed rather uniformly in the retina [D. J. Vitek, J. D. Schall, A. G. Leventhal, *J. Comp. Neurol.* **241**, 1 (1985); A. G. Leventhal, R. W. Rodieck, B. Dreher, *ibid.* **237**, 216 (1985)], provide the major input to the auditory pathway in lesioned ferrets [(*4*); A. W. Roe, P. E. Garraghty, M. Sur, *Soc. Neurosci. Abstr.* **13**, 1023 (1987); S. L. Pallas, J. Hahm, M. Sur, *ibid.* **15**, 495 (1989)]. In primary visual cortex of primates and carnivores [P. M. Daniel and D. Whitteridge, *J. Physiol. (London)* **159**, 203 (1961); R. Tusa, L. Palmer, A. Rosenquist, *J. Comp. Neurol.* **177**, 213 (1978); (*17*)], cortical magnification decreases approximately inversely with distance from central retina to the periphery, implying a logarithmic mapping of the retina on cortex.
11. Mapping indices for three other animals that were mapped extensively are (azimuth, elevation indices for each animal): 0.154 (±0.046), 0.252 (±0.079); 0.063 (±0.032), 0.278 (±0.101); 0.142 (±0.081), and 0.236 (±0.147). The correlation coefficients for the animals are (azimuth, elevation coefficient for each animal): 0.66, −0.39; 0.36, 0.35; and 0.95, 0.80. Magnification functions are very similar in different animals.
12. J. G. Kelly, P. W. Judge, D. P. Phillips, *Hear. Res.* **24**, 111 (1986).
13. Integrative properties appear to be represented along the isofrequency axis, such as discrete clusters of neurons related to EE or EI interactions between the two ears [T. J. Imig and J. Brugge, *J. Comp. Neurol.* **182**, 637 (1978); P. W. Judge and J. B. Kelly, *Soc. Neurosci. Abstr.* **14**, 651 (1988)] and the bandwidth of spectral tuning [M. L. Sutter and C. E. Schreiner, *ibid.* **15**, 1116 (1989)].
14. R. A. Andersen, P. L. Knight, M. M. Merzenich, *J. Comp. Neurol.* **194**, 663 (1980); S. Brandner and H. Redies, *J. Neurosci.* **10**, 50 (1990); (*15*). The pattern of projections from the auditory thalamus to auditory cortex in normal ferrets is very similar (*6*).
15. J. C. Middlebrooks and J. M. Zook, *J. Neurosci.* **3**, 203 (1983).
16. Our physiological mapping data (unpublished) suggest that retinal projections to the auditory thalamus are organized topographically. The projections from auditory thalamus to primary auditory cortex are as indicated in Fig. 2.
17. M. I. Law, K. R. Zahs, M. P. Stryker, *J. Comp. Neurol.* **278**, 157 (1988); A. W. Roe, S. L. Pallas, J.-O. Hahm, M. Sur, unpublished observations.
18. There are two ways by which thalamocortical projections can be widespread along the anteroposterior dimension of cortex in normal animals: (i) single thalamic cells have cortical arbors that are widespread along the anteroposterior dimension but restricted along the mediolateral dimension of cortex; and (ii) single thalamic cells have uniform cortical arbors, but cells close together have terminal fields that are widely dispersed along the anteroposterior dimension in cortex. It is possible that visual input alters either of these projection patterns in subtle ways in lesioned ferrets compared to normal ferrets.
19. D. N. Mastronarde, *J. Neurophysiol.* **49**, 303 (1983); D. Arnett and T. E. Spraker, *J. Physiol. (London)* **317**, 29 (1981); M. Meister, R. O. L. Wong, D. A. Baylor, C. J. Shatz, *Invest. Ophthalmol. Visual. Sci.* **31**, 115 (1990); L. Maffei and L. Galli-Resta, *Proc. Natl. Acad. Sci. U.S.A.* **87**, 2861 (1990).
20. We consider input selection to occur by a change in the weights of thalamocortical or intracortical synapses [M. Sur, S. L. Pallas, A. W. Roe, *Trends Neurosci.* **13**, 227 (1990)].
21. M. M. Merzenich, W. M. Jenkins, J. C. Middlebrooks, in *Dynamic Aspects of Neocortical Function*, G. M. Edelman, W. E. Gall, W. M. Cowan, Eds. (Wiley, New York, 1984), pp. 397–424.
22. Evidence from reorganization of maps after lesioning portions of peripheral input suggests that maps in both somatosensory cortex [M. M. Merzenich, G. Recanzone, W. M. Jenkins, T. T. Allard, R. J. Nudo, in *Neurobiology of Neocortex*, P. Rakic and W. Singer, Eds. (Wiley, New York, 1988), pp. 41–67] and visual cortex [J. H. Kaas *et al.*, *Science* **248**, 229 (1990)] are dynamically maintained.
23. We thank P. E. Garraghty for assisting in some experiments, T. Sullivan for assistance with histology, and P. Katz for comments on the manuscript. Supported by NIH grant EY07719 and by grants from the McKnight Foundation and the March of Dimes.

23 May 1990; accepted 10 September 1990

Analysis of Junctional Diversity During B Lymphocyte Development

KATHERYN MEEK

Immunoglobulin rearrangement is central to generating antibody diversity because of heterogeneity generated during recombination by deletion or addition of nucleotides at coding joints by the recombinase machinery. Examination of these junctional modifications revealed that the addition of nongermline-encoded nucleotides was more prevalent in adult versus fetal B cells, thus partially limiting the fetal antibody repertoire. In contrast, deletion of nucleotides occurs equivalently in B cells at different stages of development and at different points in B cell ontogeny. Finally, the bias in murine immunoglobulins for one D_H segment reading frame occurs at the D_HJ_H intermediate.

CRYSTAL STRUCTURES OF ANTIGEN-specific antibody molecules show that the hypervariable regions of the immunoglobulin heterodimer are integral to antigen binding (*1*)—thus variations in these regions engender different antigen specificities. Generally, the most variable portion is the third complementarity determining region (CDR3) (*2*).

The variation in CDR3 is generated by deletion of nucleotides from the coding sequences (presumably by an exonuclease associated with the recombinase machinery) and addition of nucleotides at the joints (N segments) in an apparently random fashion, probably by the enzyme terminal transferase (Tdt) (*3–9*). Though the rearrangement process is ostensibly random, in expressed immunoglobulins there is a preference for chains that have rearranged such that one particular D_H segment reading frame is used.

In this report, newborn and adult B cell receptors were examined for differences in junctional diversity. To analyze deletion of nucleotides from coding segments, I used the restriction enzyme sites that occur near the recombination signal sequences in various immunoglobulin gene segments (*10–14*). By digesting polymerase chain reaction (PCR)–amplified rearrangements with the appropriate restriction enzyme, the proportion of rearrangements that lacked that particular enzyme site was determined. Because in most situations the amplified rearrangements were not subject to antigenic selection (that is, D_HJ_H rearrangements or pseudogenes), the absence of the enzyme site should reflect the proportion of rearrangements that no longer contained the particular enzyme site because of nucleotide deletion during rearrangement.

Department of Internal Medicine, Division of Rheumatology, University of Texas Southwestern Medical Center, Dallas, TX 75235.